

Quinol-4-ones as Steroid A-Ring Mimetics in Nonsteroidal Dissociated Glucocorticoid Agonists

John Regan,*[†] Thomas W. Lee,[†] Renée M. Zindell,[†] Younes Bekkali,[†] Jörg Bentzien,[†] Thomas Gilmore,[†] Abdelhakim Hammach,[†] Thomas M. Kirrane,[†] Alison J. Kukulka,[†] Daniel Kuzmich,[†] Richard M. Nelson,[†] John R. Proudfoot,[†] Mark Ralph,[†] Josephine Pelletier,[‡] Donald Souza,[‡] Lijiljana Zuvella-Jelaska,[‡] Gerald Nabozny,[‡] and David S. Thomson[†]

Departments of Medicinal Chemistry and Immunology & Inflammation, Boehringer Ingelheim Pharmaceuticals, 900 Ridgebury Road, Ridgefield, Connecticut 06877

Received October 31, 2006

We report on the nuclear receptor binding affinities, cellular activities of transrepression and transactivation, and anti-inflammatory properties of a quinol-4-one and other A-ring mimetic containing nonsteroidal class of glucocorticoid agonists.

Introduction

During the past 50 years the successful treatment of inflammatory diseases has relied on the use of glucocorticoid (GC)^a agonists such as dexamethasone (**1a**) and prednisolone (**1b**) (Chart 1). While effective in controlling asthma,¹ rheumatoid arthritis,² and other disorders, GC therapy is fraught with a number of severe side effects. The seriousness of the complications often hampers high dose and chronic administration. In addition, cross reactivity with other steroid hormone receptors, such as progesterone receptor (PR) and mineral corticoid receptor (MR), of the commonly prescribed GCs can provoke off-target pharmacology. In direct response to the current state of GC therapy, finding drugs with good anti-inflammatory properties and reduced side effects remains an ongoing quest.

The probability of identifying a GC agonist with a better safety profile compared to existing therapies has substantially increased with newer understandings of the molecular mechanism of action.^{3–8} After an agonist enters a target cell and binds to the glucocorticoid hormone receptor (GR), the ligand-activated complex (GRC) translocates into the nucleus where direct and indirect functional pathways can be accessed. Acting directly, the GRC serves as an endogenous transcription factor by binding to specific DNA sequences and coactivator proteins, thereby initiating transcription of metabolic and endocrine genes. GRC-mediated transactivation of these genes is believed to contribute to the side effect profile of GC therapy.⁹ Acting indirectly, the GRC adopts a conformation with an affinity for transcription factors (e.g., NF- κ B and AP-1). Subsequent binding to these transcription factors results in the inhibition of expression of pro-inflammatory cytokines such as TNF- α and IL-6. This process, known as transrepression, is thought to contribute, in part, to the anti-inflammatory component of GCs.

Therefore, the search for GC agonists with a dissociated profile (greater transrepression than transactivation activity) has accelerated in recent years^{10,11} with an appreciation of the complex molecular pathways and the anticipation of an improved safety margin.^{12,13}

A primary objective in our GC agonist anti-inflammatory program is identifying nonsteroidal anti-inflammatory agents with the added benefit of exhibiting dissociation. Toward this end, we sought to discover pharmacophores capable of playing the hydrogen bond acceptor's role of the C-3 carbonyl of dexamethasone that could be combined with a nonsteroidal scaffold. Dissociated GC agonists **2a** and **2b**¹⁴ represent a good starting point for such a venture as they contain a benzoxazinone group as a readily replaceable A-ring mimetic.^{15,16} Other important features include the alcohol as a steroidal C-11 hydroxy surrogate, a trifluoromethyl substituent to maintain agonist activity,¹⁷ and a phenyl ring which is believed to reside adjacent to the area of steroid D-ring binding in the glucocorticoid receptor–ligand binding domain (GR–LBD). Expanding the scope of this effort to include modifications to the phenyl ring provides an opportunity to gauge whether changes to this region of the scaffold are a viable option to attenuate nuclear receptor potency and selectivity, as well as transrepression or transactivation pathways. We envision preparing the target molecules, represented by **5**, by the opening of epoxide **3** (Chart 1) with a nucleophilic amine embedded in a lipophilic ring containing a hydrogen bond acceptor functionality¹⁸ (i.e., atom A in **4**). The syntheses and biological profiles of compounds such as **5** are the subject of this paper.

Chemistry

The preparations of a quinol-4-one-containing analogue (**11**) and a piperid-4-one (**14**) are shown in Scheme 1 as representative examples of **5**. The key step in this sequence is the opening of an epoxide (i.e., **9**) with a nucleophilic amine. Briefly, the preparation of epoxide **9** begins with the copper-mediated 1,4-addition of Grignard reagent **6** to 1,1,1-trifluorobut-3-en-2-one (**7**)¹⁹ to provide ketone **8**. Trimethylsulfoxonium iodide and NaH transform **8** to epoxide **9**. Quinolone **11** is obtained by reacting **9** with 4-hydroxyquinoline (**10**) and sodium ethoxide in ethanol.²⁰ Conversion of the methoxy group in **11** to a hydroxy in **12** is accomplished with BBr₃. Piperidin-4-one analogue **14** is prepared from the reaction of **9**, *cis*-3,5-dimethyl-4-piperidone hydrochloride (**13**)^{21,22} and K₂CO₃ in DMF.

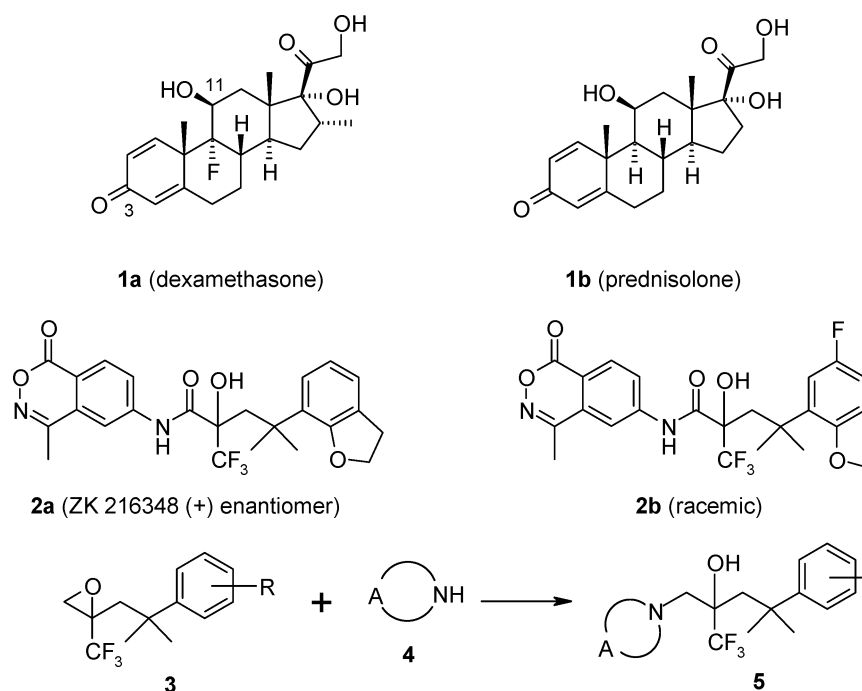
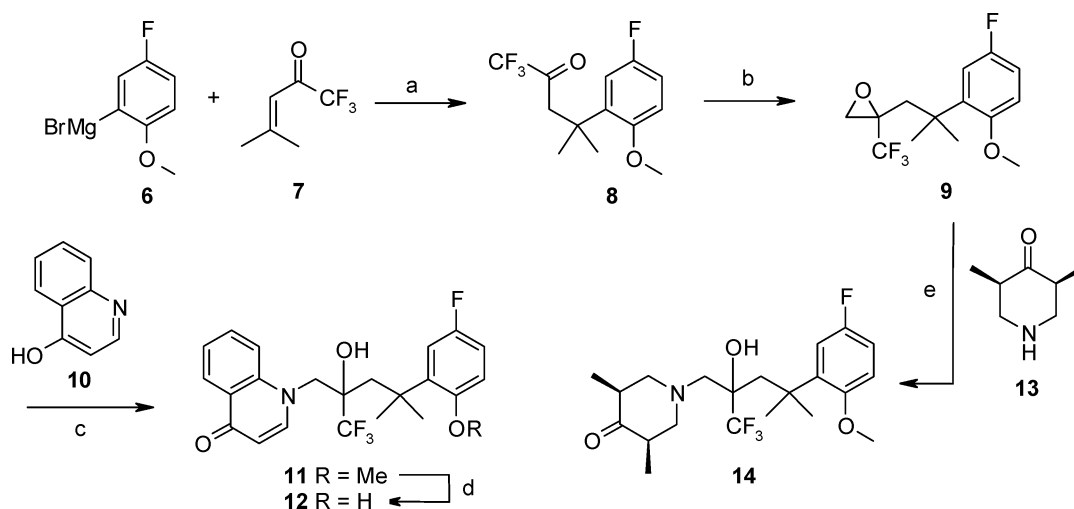
* To whom correspondence should be addressed. Phone: (203) 798-4768. Fax: (203) 791-6072. E-mail: jregan@rdg.boehringer-ingelheim.com.

[†] Department of Medicinal Chemistry.

[‡] Department of Immunology & Inflammation.

^a Abbreviations: AP-1, activator protein-1; DBF, dihydrobenzofuran; DELFIA, dissociation-enhanced lanthanide fluorescent immunoassay; DMEM, Dulbecco's modified Eagle's medium; D-gal, D-galactose; CHAPS, 3-[(3-cholamidopropyl)dimethylammonio]-1-propanesulfonate; EDTA, ethylenediaminetetraacetic acid; ELISA, enzyme-linked immunosorbent assay; FP, fluorescence polarization; GC, glucocorticoid; GRC, glucocorticoid receptor–ligand complex; GR, glucocorticoid receptor; GR–LBD, glucocorticoid receptor–ligand binding domain; HFF, human foreskin fibroblast; HSP, heat-shock protein; IL-6, interleukin-6; LPS, lipopolysaccharide; MMTV, mouse mammary tumor virus; MR, mineral corticoid receptor; NF, nuclear factor; PR, progesterone receptor; TES, *N*-[tris(hydroxymethyl)methyl]-2-aminoethanesulfonic acid; TNF- α , tumor necrosis factor- α .

Chart 1

Scheme 1^a

^a Reagents and conditions: (a) CuI (1.1 equiv)/THF, $-20\text{ }^{\circ}\text{C}$, 30 min, then **7** (1.1 equiv), room temperature overnight; (b) trimethylsulfoxonium iodide/NaH/DMSO; (c) **10**/NaOEt/ethanol, heat; (d) BBr_3 (10 equiv)/ CH_2Cl_2 , room temperature overnight; (e) **13** (2 equiv)/ K_2CO_3 (5 equiv)/DMF, $100\text{ }^{\circ}\text{C}$, 1.5 h.

Results and Discussion

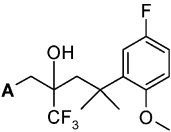
The nuclear receptor binding potency of the target compounds is determined by their ability to compete for receptor binding with tetramethylrhodamine-labeled dexamethasone (GR, MR) or mifepristone (PR).²³ The transrepression potential is measured in human foreskin fibroblast (HFF) cells. Inhibition of IL-1 stimulated IL-6 production, and the percent efficacy is compared with that of dexamethasone.^{24,25} In an effort to establish transactivation activity, compounds are counterscreened for the induction of aromatase in HFF cells²⁶ and the ability to activate the MMTV promoter in HeLa cells transfected with an MMTV luciferase construct.²⁷ Comparisons with dexamethasone establish a basis for identifying compounds with a dissociated profile.

Table 1 shows the effects of A-ring replacements in scaffold **5**. Morpholine **15**, pyridin-4-one **17**, and imidazole **18** are devoid of activity, while piperidin-4-one **16** demonstrates weak GR binding affinity ($\text{IC}_{50} = 1400\text{ nM}$). Introducing methyl groups on the ring is an opportunity to increase the lipophilicity and

perhaps provide a water shield to the hydrogen bond network consisting of the A-ring mimetic acceptor and the GR-LBD donor. The outcome is a significant enhancement in GR binding affinity. For example, *cis*-dimethylpiperidin-4-one **14** exhibits a 140-fold gain in GR binding ($\text{IC}_{50} = 10\text{ nM}$). Other methylated analogues include *cis*-dimethylmorpholine **20**, dimethylpyridin-4-one **21**, and dimethylimidazole **22** with IC_{50} values of 38, 120, and 650 nM, respectively. Introducing methyl groups onto the A-ring replacements has no effect on PR binding affinity, whereas modest activity against MR is seen. In the transrepression anti-inflammatory cellular assay, compounds **14** and **21** inhibit IL-6 release from HFF with IC_{50} values of 75 and 53 nM, respectively, and 87–89% efficacy compared to dexamethasone.

Further increasing the lipophilicity of the A-ring mimetic from methyl substitutions to fusing an aromatic nucleus to the hydrogen bond acceptor ring provides analogues shown in Table 2. Changes in GR binding avidity with this modification vary

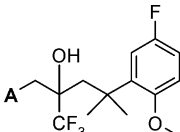
Table 1. Methyl-Substituted A-Ring Mimetics



Cmpd. No.	A	GR ^a IC ₅₀ (nM)	PR ^a IC ₅₀ (nM)	MR ^a IC ₅₀ (nM)	IL-6 Inhib. in HFF ^b IC ₅₀ (nM) and efficacy (% vs. dex.)	Cmpd. No.	A	GR ^a IC ₅₀ (nM)	PR ^a IC ₅₀ (nM)	MR ^a IC ₅₀ (nM)	IL-6 Inhib. in HFF ^b IC ₅₀ (nM) and efficacy (% vs. dex.)
1a (Chart 1)		3	>2,000	33	0.51 (100%)	18		>2,000	>2,000	>2,000	nt
2a (Chart 1)		3	19	38	59 (80%)	19		110	>2,000	1,500	>2,000 (41%)
2b (Chart 1)		8	22	130	>2,000 (19%)	20		38	>2,000	450	270 (72%)
14		10	>2,000	430	75 (89%)	21		120	>2,000	1,900	53 (87%)
15		>2,000	>2,000	>2,000	nt ^c	22		650	>2,000	620	nt
16		1,400	>2,000	>2,000	nt						
17		>2,000	>2,000	>2,000	nt						

^a IC₅₀ values were determined from duplicate 11-point concentration–response curves. See ref 23. ^b IC₅₀ values represent the mean of at least two independent determinations. See ref 25. ^c Not tested.

Table 2. Phenyl-Fused A-Ring Mimetics



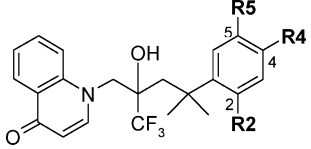
Cmpd. No.	A	GR ^a IC ₅₀ (nM)	PR ^a IC ₅₀ (nM)	MR ^a IC ₅₀ (nM)	IL-6 Inhib. in HFF ^b IC ₅₀ (nM) and efficacy (% vs. dex.)	Cmpd. No.	A	GR ^a IC ₅₀ (nM)	PR ^a IC ₅₀ (nM)	MR ^a IC ₅₀ (nM)	IL-6 Inhib. in HFF ^b IC ₅₀ (nM) and efficacy (% vs. dex.)
11		10	470	120	21 (82%)	26		54	>2,000	775	>2,000 (15%)
23		15	640	310	600 (25%)	27		690	>2,000	>2,000	nt
24		4	90	130	110 (72%)	28		77	>2,000	1,100	56 (78%)
25		950	>2,000	1,600	nt ^c	29		34	>2,000	175	35 (72%)

^a IC₅₀ values were determined from duplicate 11-point concentration–response curves. See ref 23. ^b IC₅₀ values represent the mean of at least two independent determinations. See ref 25. ^c Not tested.

between 2- and 10-fold. For example, compare **14** with **24**, **22** with **26**, and **21** with **11**. However, of these compounds, only quinolone **11** potently inhibits cellular IL-6 production (IC₅₀ = 21 nM and 82% efficacy). These results reinforce the often observed lack of correlation between GR binding affinity and

transrepression activity.^{10,28,29} A likely explanation is that the flexibility of the GR–LBD can accommodate these ligands but, in doing so, is rendered incapable of effectively interacting with anti-inflammatory transcription factors.^{30,31} Support for the critical role of the hydrogen bond accepting atom in the A-ring

Table 3. Phenyl Ring Modifications



compd no.	R2	R4	R5	GR IC ₅₀ ^a (nM)	PR IC ₅₀ ^a (nM)	MR IC ₅₀ ^a (nM)	IL-6 inhib in HFF IC ₅₀ ^b (nM) (efficacy, % vs dexamethasone)
11	OMe	H	F	10	475	120	27 (82)
12	OH	H	F	5	960	580	6 (92)
30	H	H	H	28	106	350	78 (48)
31	OH	H	H	6	555	450	6 (90)
32	Me	H	H	22	240	150	61 (63)
33	Me	H	F	10	240	120	34 (66)
34	OH	H	Me	8	160	160	5.6 (93)
35	Me	H	OMe	11	525	91	17 (86)
36	Me	H	OH	780	>2000	>2000	nt ^c
37	OH	F	H	3	340	880	3 (88)
38 ^d				4	48	98	11 (86)

^a IC₅₀ values were determined from duplicate 11-point concentration–response curves. See ref 23. ^b IC₅₀ values represent the mean of at least two independent determinations. See ref 25. ^c Not tested. ^d See Table 5 for the structure.

replacements is highlighted with tetrahydroquinoline **25**. A factor of 200 decrease in GR binding affinity, compared to that of dihydroquinolone **24**, underscores the importance of achieving a hydrogen bond network in the GR–LBD with this series. The 3-fold difference in GR binding affinity between benzo[1,4]-oxazine **23** and dihydroquinolone **24** may reflect a stronger hydrogen bond acceptor pharmacophore and an advantageous distance for **24** between the hydrogen bond donor of the protein and the acceptor group on the ligand. One consequence of fusing a phenyl ring to this scaffold is an erosion of the GR/PR ratio from greater than 75-fold for compounds without a fused aromatic nucleus (**14** and **20**) to less than 50-fold for those with a phenyl ring attached (**11**, **23**, **24**). The GR/MR binding ratio was nearly unchanged. Interestingly, benzimidazole **26** does not show a loss of nuclear receptor selectivity. Additional changes to the A-ring mimetic involve embedding a nitrogen atom into the aromatic nucleus as a goal to define polarity limits. Table 2 describes the consequences of a quinazolinone (**27**) and naphthyridin-4-ones (**28**, **29**) acting as A-ring replacements. Compared to **11**, a significant diminution in GR binding is observed for **27** and less so with **28** and **29**. Nevertheless, both **28** and **29** retain satisfactory transrepression activity. These data suggest the lipophilic environment of the A-ring binding domain in GR can tolerate ligands with somewhat increased polarity whereas the PR–LBD does not readily accommodate these changes. Of the phenyl-fused A-ring replacements shown in Table 2, compounds **11**, **23**, **24**, **26**, **28**, and **29** achieve the highest GR binding affinity, but only **11**, **28**, and **29** reach IC₅₀ values <100 nM in the transrepression assay.

Molecular modeling suggests that, upon binding to the GR–LBD, the phenyl ring of **2b** resides adjacent to the steroid D-ring domain.^{15,16} The contribution to GR binding and transrepression activity of simple groups attached to the phenyl ring in the quinolone-containing scaffold is summarized in Table 3. Conversion of the methoxy group at C-2 (**11**, R2 = OMe) to a hydroxy (**12**, R2 = OH) improves the transrepression activity. Removal of the hydroxy group and fluorine atom from **12** (compound **30**) weakens the GR binding affinity (IC₅₀ = 28 nM) and decreases the agonist activity in the cellular assay (IC₅₀ = 78 nM and 48% efficacy). Also seen is a decline in the GR/PR ratio. Maintaining only a hydroxy group (**31**) restores the binding (GR IC₅₀ = 6 nM) and cellular activity (IC₅₀ = 6 nM

and 90% efficacy). In addition, a good GR/PR binding ratio is re-established. Switching the hydroxy group at C-2 to a methyl (i.e., R2 = Me, **32** and **33**) maintains the GR binding affinity but lessens the GR/MR ratio. Reductions in IL-6 inhibition (IC₅₀ values of 30–60 nM) and lower efficacies are also observed (63–66%) for this change. Substituting an electronegative atom at C-5 for an electropositive atom (**34**) retains the GR binding and cellular activity with an increase in PR and MR binding affinities compared to those of **12**. Further changing the electronic character at C-5 by introducing a methoxy improves the agonist activity compared to that of **33**. However, placing a hydroxy group at C-5 (**36**) causes a significant loss of GR binding, implying a negative interaction of a hydrogen bond donor at this site. Phenyl ring analogues involving substitution at C-4 reveal a very narrow range of acceptable pharmacophores. Only fluorine at this site provides good GR binding affinity and cellular activity (**37**). Groups larger than fluorine (methyl, methoxy, hydroxy) generally lead to a significant loss of binding affinity (data not shown). Incorporating the oxygen atom at C-2 into a dihydrobenzofuran (DBF) ring (**38**) significantly diminishes the nuclear receptor selectivity. The transrepression activity is comparable to that of **11**. The above survey of substituents on the phenyl ring of the quinolone-containing steroid mimetic generally demonstrates a range of nuclear receptor binding affinity smaller than a factor of 10. However, pharmacophores such as methoxy or hydroxy at C-2 (**11**, **12**, **31**, **34**, and **37**) and DHB (**38**) are required for achieving the best agonist profile. Another general trend (data not shown) for this series is a hydroxy group at C-2 displays better IL-6 inhibition and efficacy compared to a methoxy despite similar GR binding affinities (e.g., **11** vs **12**). Also important are the substitution patterns at C-2 and C-5 (**34** vs **35**) and steric constraints at C-4. Taken together, these results highlight the important relationships of size and polarity required for favorable interactions adjacent to the steroid D-ring domain within the GR–LBD. In addition, similar observations are noted with phenyl ring substitutions for molecules containing A-ring mimetics other than quinol-4-one. See Table 5 for examples.

A primary goal of this project is identifying GC agonists that can distinguish between transrepression and transactivation pathways. Two assays are used as a counterscreen to determine the extent of transactivation. Dexamethasone activates the MMTV promoter in HeLa cells transfected with an MMTV luciferase construct. In addition, dexamethasone induces expression of aromatase in HFF.³² Several compounds were evaluated for their transactivation potential to activate MMTV and induce aromatase expression (EC₅₀ and percent efficacy). A compound can be characterized as dissociated with either weak activity or low efficacy, or both, in the transactivation assays compared to the transrepression assay. The role that phenyl ring substitutions play in defining dissociation is seen in Table 4. In the MMTV assay, 2-hydroxyphenyl compounds **12** and **37** are partial agonists (EC₅₀ = 15–37 nM and 20–35% efficacy) while the other compounds are devoid of activity compared to dexamethasone. In the aromatase induction assay, **12** and **37** exhibit pronounced activity with EC₅₀ = 15–17 nM and 65–74% efficacies. Alternatively, 2-methoxyphenyl, 2-methylphenyl, and DBF analogues (**11**, **32**, and **38**) display low potency or efficacy in the aromatase assay. Of the modifications at C-5 of the phenyl ring, methoxy **35** displays moderate activity against aromatase (EC₅₀ = 95 nM, 65% efficacy) while hydrogen or fluorine (**32** and **33**) are weakly potent and efficacious derivatives. These data suggest groups on the phenyl ring have an important influence on the degree of dissociation and parallel the observa-

Table 4. Dissociation Profiles

compd no.	GR IC ₅₀ ^a (nM)	IL-6 inhib in HFF IC ₅₀ ^b (nM) (efficacy, % vs dexamethasone)	MMTV activation in HeLa EC ₅₀ ^c (nM) (efficacy, % vs dexamethasone)	aromatase inhib in HFF EC ₅₀ ^d (nM) (efficacy, % vs dexamethasone)
1a	3.4	0.5 (100)	17 (100)	1.9 (100)
1b	15	6.6 (96)	16 (91)	19 (92)
2a	3	59 (80)	>2000 (14)	91 (56)
11	10	27 (82)	>2000 (10)	220 (67)
12	5	6 (92)	37 (20)	14 (74)
14	10	75 (89)	nt ^e	240 (93)
21	120	53 (87)	>2000 (3)	170 (77)
28	77	56 (78)	nt	ip ^f (41)
29	34	35 (72)	>2000 (1)	ip (39)
32	22	61 (63)	>2000 (1)	>2000 (29)
33	10	34 (66)	>2000 (2)	ip (22)
35	11	17 (86)	>2000 (6)	95 (65)
37	3	3 (88)	15 (35)	17 (82)
38^g	4	11 (86)	nt	ip (60)
39^g	34	39 (77)	nt	ip (26)
40^g	48	47 (59)	nt	>2000 (14)
41^g	125	70 (71)	nt	>2000 (20)

^a IC₅₀ values were determined from duplicate 11-point concentration–response curves. See ref 23. ^b IC₅₀ values represent the mean of at least two independent determinations. See ref 25. ^c EC₅₀ values represent the mean of at least two independent determinations. See ref 27. ^d EC₅₀ values represent the mean of at least two independent determinations. See ref 26. ^e Not tested. ^f Due to the flat shape of the dose–response curve, an EC₅₀ value beyond 2000 nM could not be calculated. ^g See Table 5 for the structures.

tion that some steroids containing modified D-rings show dissociated activities.³³ The contribution of the A-ring replacement to the dissociation profile is seen in Table 4. Comparing compounds with the 2-methoxy-5-fluorophenyl ring, dimethylpiperidin-4-one **14**, dimethylpyridin-4-one **21**, and naphthyridin-4-one **28** demonstrate a somewhat weaker transactivation response compared to quinol-4-one **12**. However, the 2-methyl-5-fluorophenyl and DBF rings impart a much more dissociated profile for dimethylpyridin-4-one (**39** and **41**), naphthyridin-4-one (**40**), and quinol-4-one (**33** and **38**) A-ring mimetics. Thus, a distinction between potent transrepression activity and diminished transactivation is achieved with the proper choice of A-ring replacements and phenyl substitution with this class of compounds.

Selected dissociated compounds were evaluated for their anti-inflammatory properties in an LPS-stimulated mouse model of TNF- α production. Test compounds were administered orally in Cremophor 60 min prior to LPS challenge. TNF- α levels were measured 60 min later. Table 5 summarizes the GR binding and cellular and in vivo transrepression profiles of various combinations of A-ring (dimethylpyridin-4-one, quinol-4-one, and naphthyridin-4-one) and phenyl ring analogues. When dosed at 10 mg/kg, the nondissociated analogue **12** and dissociated compounds **33** and **38–41** inhibit TNF- α production (48–58%).

Conclusion

Several new types of pharmacophores can serve as A-ring mimetics with good binding affinity for GR for this scaffold. These include dimethylpiperidin-4-one (**14**), quinolone (**11**), *cis*-dimethylmorpholine (**20**), benzo[1,4]oxazine (**23**), dihydroquinolone (**24**), benzimidazole (**26**), and naphthyridin-4-one (**29**). In addition, good nuclear receptor selectivity is achieved. Of these, **11**, **29**, and dimethylpyridin-4-one (**21**) exhibit good transrepression activity in a cellular assay of IL-6 production. The substitution patterns on the phenyl ring play an important role in defining GR binding affinity and the degree of transrepression. Compounds with a hydroxy group at C-2 obtain the highest efficacy levels of transrepression, while a C-5 hydroxy is deleterious toward activity. Methyl and methoxy substituents

Table 5. In Vivo Activities of Dissociated Agonists

12, 32, 33, 38-41

A =

phenyl ring =

compd no.	A	phenyl ring	GR IC ₅₀ ^a (nM)	IL-6 inhib in HFF IC ₅₀ ^b (nM) (efficacy, % vs dexamethasone)	inhib of TNF- α in mice ^c (%) (<i>n</i> = 8) (10 mg/kg)
1b^d	see Chart 1		15	7 (96)	84 \pm 8
12	see Table 3		5	6 (92)	55 \pm 6
32	II	II	22	61 (63)	36 \pm 10
33	II	I	10	34 (66)	50 \pm 17
38	II	III	4	11 (86)	49 \pm 10
39	I	III	34	39 (77)	49 \pm 6
40	III	I	48	47 (59)	58 \pm 12
41	I	I	125	70 (71)	48 \pm 11

^a IC₅₀ values were determined from duplicate 11-point concentration–response curves. See ref 23. ^b IC₅₀ values represent the mean of at least two independent determinations. ^c See the Experimental Section. ^d 3 mg/kg, po.

at C-2 and C-5 are well tolerated. The dissociated profile of this series in either the MMTV or aromatase assays was dependent upon the choice of the A-ring mimetic and the substitution on the phenyl ring. As A-ring replacements, fused rings **11**, **28**, and **29** exhibit a superior dissociated profile due to differences in either potency or efficacy in the transactivation assays compared to monocyclic rings **14** and **21**. In general, methyl and methoxy groups at C-2 of the phenyl ring demonstrate weaker transactivation activities than hydroxy at this site. In an animal model of inflammation, compounds **12**, **33**, and **38–41** potently inhibit TNF- α production. Thus, the nuclear receptor binding affinities, the cellular levels of transrepression and transactivation, and the anti-inflammatory properties have been demonstrated with the quinol-4-one-containing class of GR agonists. Further work in this series will be reported in due course.

Experimental Section

All solvents and reagents were obtained from commercial sources and used without further purification. Flash chromatography was performed according to the procedure of Still et al. (EM Science Kieselgel 60, 70–230 mesh). Melting points were obtained from a Mel-temp 3.0 or Fisher-Johns melting point apparatus and are uncorrected. The ¹H NMR spectra were recorded on a Bruker DPX 400 spectrometer. Chemical shifts are reported in parts per million (δ) from the tetramethylsilane resonance in the indicated solvent. Infrared spectra were recorded without solvent on a Nicolet Impact 410. Mass spectra were obtained from a Finnigan-SSQ7000 spectrometer. Samples were generally introduced by a particle beam and ionized with NH₄Cl. The analytical HPLC purity was established with the following protocols. Method A: Gilson chromatographic system, Waters SureFire reversed-phase C₁₈ analytical column (4.6 \times 50 mm, 5 μ m, part number 186002557), flow rate 5 mL/min, detection with a Gilson UV/VIS-155 at 254 nm, sample

size 25 μL , gradient 5% acetonitrile in water with 0.1% TFA to 95% acetonitrile in water with 0.1% TFA over 6 min and held. Method B: Rainin chromatography system, model SD-200, Tosoh Bioscience TSK Super ODS column (4.6 mm \times 10 cm, 2 μM , part number G0030-90F), flow rate 1.2 mL/min, detection with Dynamax absorbance detector at 254 nm, gradient 5% acetonitrile in water with 0.05% TFA to 95% acetonitrile in water with 0.05% TFA over 10 min and held. Method C: Rainin chromatography system, model SD-200, Whatman PartiSphere C-8 column (4.6 \times 125 mm, 5 μm , part number 4621-0503), detection with Dynamax absorbance detector at 254 nm, gradient 5% acetonitrile in water with 0.1% TFA to 95% acetonitrile in water with 0.1% TFA.

1,1,1-Trifluoro-4-methylpent-3-en-2-one (7). To a 0–5 $^{\circ}\text{C}$ mixture of *N,O*-dimethylhydroxylamine hydrochloride (15.8 g) in CH_2Cl_2 (400 mL) was added dropwise trifluoroacetic anhydride (21.7 mL). Pyridine (37 mL) was added to the mixture dropwise. The resulting mixture was stirred at 0–5 $^{\circ}\text{C}$ for 0.5 h and diluted with water. The organic layer was washed with water, 1 N aqueous HCl, water, and brine and dried (MgSO_4). Removal of the volatiles in vacuo for 5 min provided 2,2,2-trifluoro-*N*-methoxy-*N*-methylacetamide as a colorless oil.

To a 0–5 $^{\circ}\text{C}$ mixture of 2,2,2-trifluoro-*N*-methoxy-*N*-methylacetamide (3 g) in 30 mL of anhydrous ether was added (2-methylpropenyl)magnesium bromide in THF (42 mL of a 0.5 M solution). The reaction was stirred at 0–5 $^{\circ}\text{C}$ for 0.5 h, warmed to room temperature, and stirred overnight. The reaction was quenched with saturated aqueous NH_4Cl and extracted with ether three times. The organic layers were combined, washed with water and brine, and dried (MgSO_4). Most of the volatiles were removed at atmospheric pressure, providing **7** as an approximately 75% pure solution containing ether and THF that was used without further purification.

1,1,1-Trifluoro-4-(5-fluoro-2-methoxyphenyl)-4-methylpentan-2-one (8). To a 0–5 $^{\circ}\text{C}$ solution of **7** (24 g, approximately 75% pure solution containing ether and THF) and CuI (30.1 g) in ether (300 mL) was added (5-fluoro-2-methylphenyl)magnesium bromide (315 mL, 157 mmol, 0.5 M solution in THF). The mixture was warmed to room temperature, stirred overnight, and diluted with saturated aqueous NH_4Cl (15 mL) and ethyl acetate. The organic layer was washed with water and brine and dried (MgSO_4). Removal of the volatiles in vacuo provided a residue which was purified by flash silica gel chromatography using 0–5% ethyl acetate in hexanes as the eluent. The product-rich fractions were collected and the volatiles removed in vacuo to yield 20.3 g (46%) of **8** as an oil.

2-[2-(5-Fluoro-2-methoxyphenyl)-2-methylpropyl]-2-(trifluoromethyl)oxirane (9). To a suspension of trimethylsulfoxonium iodide (4.76 g, 21.5 mmol) in DMSO (25 mL) was added NaH (0.863 g of a 60% dispersion in oil, 21.5 mmol) in four portions. After being stirred for 0.5 h, the solution was added to **8** (5.00 g, 17.9 mmol) in DMSO (20 mL). After 2 h the mixture was diluted with water (150 mL) and extracted with ether (2 \times 125 mL). The combined organic layers were washed with water and brine and dried (MgSO_4). Removal of the volatiles in vacuo provided **9** as an oil which was used without further purification.

1-[4-(5-Fluoro-2-methoxyphenyl)-2-hydroxy-4-methyl-2-(trifluoromethyl)pentyl]-1*H*-quinolin-4-one (11). A mixture of **9** (0.226, 0.773 mmol), 4-hydroxyquinoline (**10**; 0.112 g, 0.773 mmol), sodium ethoxide (0.28 mL of a 21 wt % solution in ethanol, 0.77 mmol), and anhydrous ethanol (4 mL) was heated at 85 $^{\circ}\text{C}$ for 6 h, cooled to room temperature, diluted with ethyl acetate and acetic acid, washed with water and brine, and dried (MgSO_4). Removal of the volatiles in vacuo provided a residue which was purified with flash silica gel chromatography using ethyl acetate as the eluent. The product-rich fractions were collected and the volatiles removed in vacuo to yield 0.13 g (38%) of **11**. Mp: 198–200 $^{\circ}\text{C}$. ^1H NMR (400 MHz, CDCl_3): δ 8.21 (d, 1H), 7.42 (m, 2H), 7.25 (s, 1H), 7.1 (m, 1H), 6.92 (m, 2H), 6.80 (m, 1H), 4.15 (dd, 2H), 3.80 (s, 3H), 2.55 (dd, 2H), 1.5 (s, 3H), 1.33 (s, 3H). FTIR neat (cm^{-1}): 1624, 1610. MS (ESI): *m/e* 438 (MH^+). HPLC

purity: method A 99%, retention time (t_R) 3.53 min; method B 98%, t_R 7.98 min.

1-[4-(5-Fluoro-2-hydroxyphenyl)-2-hydroxy-4-methyl-2-(trifluoromethyl)pentyl]-1*H*-quinolin-4-one (12). To a solution of **11** (0.082 g, 0.19 mmol) in CH_2Cl_2 (3 mL) at -20 $^{\circ}\text{C}$ was added dropwise BBr_3 (1.9 mL of a 1 M solution in CH_2Cl_2 , 1.9 mmol). The mixture was stirred for 1 h and quenched with saturated NaHCO_3 and ethyl acetate. The organic layer was washed with saturated NaHCO_3 and brine and dried (MgSO_4). Removal of the volatiles in vacuo left a residue which was purified by trituration in ether and ethyl acetate and provided 0.041 g of product. Mp: 222–223 $^{\circ}\text{C}$. ^1H NMR (400 MHz, $\text{DMSO}-d_6$): δ 9.98 (s, 1H), 8.30 (d, 1H), 7.87 (d, 1H), 7.75 (t, 1H), 7.52 (t, 1H), 7.33 (m, 2H), 7.13 (m, 1H), 7.05 (m, 1H), 7.48 (s, 1H), 6.20 (d, 1H), 4.21 (m, 2H), 3.24 (d, 1H), 2.15 (d, 1H), 1.75 (s, 3H), 1.55 (s, 3H). MS (ESI): *m/e* 424 (MH^+). HPLC purity: method A 98%, t_R 3.11 min; method B 95%, t_R 7.16 min.

***cis*-1-[4-(5-Fluoro-2-methoxyphenyl)-2-hydroxy-4-methyl-2-(trifluoromethyl)pentyl]-3,5-dimethylpiperidin-4-one Hydrochloride (14).** A mixture of **9** (0.092 g, 0.32 mmol), *cis*-3,5-dimethylpiperidin-4-one hydrochloride (**13**; 0.103 g, 0.64 mmol), and powdered K_2CO_3 (0.218 g, 1.58 mmol) in DMF (3 mL) was heated at 100 $^{\circ}\text{C}$ for 1.5 h, cooled to room temperature, diluted with ether, washed thoroughly with water and brine, and dried (MgSO_4). Removal of the volatiles in vacuo provided a residue which was treated with ethereal HCl. The mixture was filtered and the solid washed with ether and dried in vacuo to provide 0.015 g of product. Mp: 77–80 $^{\circ}\text{C}$. ^1H NMR (400 MHz, CDCl_3): δ 7.02 (dd, 1H), 6.78 (m, 1H), 6.68 (m, 1H), 3.75 (s, 3H), 1.52 (s, 3H), 1.28 (s, 3H), 0.78 (d, 6H). MS (ESI): *m/e* 420 (MH^+). HPLC purity: method C 92%, t_R 10.25 min.

1,1,1-Trifluoro-4-(5-fluoro-2-methoxyphenyl)-4-methyl-2-(morpholin-4-ylmethyl)pentan-2-ol Hydrochloride (15). Mp: 195–200 $^{\circ}\text{C}$. ^1H NMR (400 MHz, CDCl_3): δ 6.97 (dd, 1H), 6.78 (m, 1H), 6.68 (m, 1H), 4.55 (s, 1H), 3.75 (s, 3H), 3.46 (br s, 4H), 2.33 (m, 4H), 2.14 (d, 2H), 1.97 (d, 2H), 1.52 (s, 3H), 1.32 (s, 3H). MS (ESI): *m/e* 380 (MH^+). HPLC purity: method A 99%, t_R 2.41 min; method B 99%, t_R 6.35 min.

1-[4-(5-Fluoro-2-methoxyphenyl)-2-hydroxy-4-methyl-2-(trifluoromethyl)pentyl]piperidin-4-one Hydrochloride (16). Mp: 134–136 $^{\circ}\text{C}$. ^1H NMR (400 MHz, $\text{DMSO}-d_6$): δ 6.8 (m, 3H), 4.55 (br s, 1H), 3.62 (s, 3H), 2.7–2.0 (m, 12H), 1.36 (s, 3H), 1.18 (s, 3H). MS (ESI): *m/e* 392 (MH^+). HPLC purity: method C 94%, t_R 7.42 min.

1-[4-(5-Fluoro-2-methoxyphenyl)-2-hydroxy-4-methyl-2-(trifluoromethyl)pentyl]-1*H*-pyridin-4-one (17). Mp: 205–206 $^{\circ}\text{C}$. ^1H NMR (400 MHz, $\text{DMSO}-d_6$): δ 7.48 (d, 2H), 7.12 (m, 3H), 6.47 (s, 1H), 6.07 (d, 2H), 3.92 (s, 3H), 3.81 (d, 1H), 3.60 (d, 1H), 2.92 (d, 1H), 2.18 (d, 1H), 1.65 (s, 3H), 1.45 (s, 3H). IR (cm^{-1}): 1639. MS (ESI): *m/e* 388 (MH^+). HPLC purity: method A 99%, t_R 2.72 min; method B 99%, t_R 6.84 min.

1,1,1-Trifluoro-4-(5-fluoro-2-methoxyphenyl)-2-(imidazol-1-ylmethyl)-4-methylpentan-2-ol (18). Mp: 166–167 $^{\circ}\text{C}$. ^1H NMR (400 MHz, CDCl_3): δ 8.1 (br s, 1H), 7.2–6.7 (m, 6H), 3.94 (dd, 2H), 3.78 (s, 3H), 2.45 (s, 2H), 1.44 (s, 3H), 1.33 (s, 3H). MS (ESI): *m/e* 361 (MH^+). HPLC purity: method A 99%, t_R 2.56 min; method B 98%, t_R 6.59 min; method C 96%, t_R 8.67 min.

2-[(*trans*-2,6-Dimethylmorpholin-4-yl)methyl]-1,1,1-trifluoro-4-(5-fluoro-2-methoxyphenyl)-4-methylpentan-2-ol Hydrochloride (19). Mp: 50–55 $^{\circ}\text{C}$. Free base ^1H NMR (400 MHz, CDCl_3): δ 7.02 (m, 1H), 6.81 (m, 1H), 6.69 (m, 1H), 4.68 (br d, 1H), 3.76 (m, 5H), 2.26 (m, 4H), 2.1–1.85 (m, 4H), 1.51 (s, 3H), 1.30 (s, 3H), 1.03 (br s, 6H). MS (ESI): *m/e* 408 (MH^+). HPLC purity: method A 99%, t_R 3.16 and 3.61 min; method B 99%, t_R 8.19 and 9.23 min.

2-[(*cis*-2,6-Dimethylmorpholin-4-yl)methyl]-1,1,1-trifluoro-4-(5-fluoro-2-methoxyphenyl)-4-methylpentan-2-ol Hydrochloride (20). Mp: 133–135 $^{\circ}\text{C}$. ^1H NMR (400 MHz, $\text{DMSO}-d_6$): δ 6.8 (m, 3H), 4.13 (br s, 1H), 3.74 (br s, 2H), 3.58 (s, 3H), 3.0–1.7 (m,

8H), 1.30 (s, 3H), 1.14 (s, 3H), 0.8 (br s, 6H). MS (ESI): *m/e* 408 (MH⁺). HPLC purity: method A 99%, *t_R* 2.76 min; method B 99%, *t_R* 6.96 min.

1-[4-(5-Fluoro-2-methoxyphenyl)-2-hydroxy-4-methyl-2-(trifluoromethyl)pentyl]-3,5-dimethyl-1H-pyridin-4-one (21). Mp: 246–247 °C. ¹H NMR (400 MHz, DMSO-*d*₆): δ 7.29 (s, 2H), 7.05 (m, 3H), 6.27 (s, 1H, OH), 3.80 (s, 3H), 3.61 (d, 1H, *J* = 15.0 Hz), 3.37 (d, 1H, *J* = 15.0 Hz), 2.80 (d, 1H, *J* = 15.6 Hz), 2.00 (d, 1H, *J* = 15.6 Hz), 1.75 (s, 6H), 1.53 (s, 3H), 1.31 (s, 3H). FTIR (neat): 1649 cm⁻¹. MS (ES): *m/e* 416 ([M + H]⁺). HPLC purity: method A 99%, *t_R* 2.95 min; method B 94%, *t_R* 7.69 min.

2-[(2,4-Dimethylimidazol-1-yl)methyl]-1,1,1-trifluoro-4-(5-fluoro-2-methoxyphenyl)-4-methylpentan-2-ol (22). Mp: 185–186 °C. ¹H NMR (400 MHz, CDCl₃): δ 7.04 (m, 1H), 6.87 (m, 1H), 6.78 (m, 1H), 6.40 (s, 1H), 3.80 (s, 3H), 3.70 (m, 2H), 2.45 (m, 2H), 2.22 (s, 3H), 2.15 (s, 3H), 1.47 (s, 3H), 1.36 (s, 3H). MS (ESI): *m/e* 389 (MH⁺). HPLC purity: method A 99%, *t_R* 2.75 min; method C 96%, *t_R* 7.04 min.

2-[(2,3-Dihydrobenzo[1,4]oxazin-4-yl)methyl]-1,1,1-trifluoro-4-(5-fluoro-2-methoxyphenyl)-4-methylpentan-2-ol (23). Mp: 98–99 °C. ¹H NMR (400 MHz, CDCl₃): δ 7.13 (dd, 1H), 6.88 (m, 1H), 6.72 (m, 1H), 6.65 (m, 1H), 6.56 (m, 2H), 5.85 (d, 1H), 4.03 (m, 2H), 3.73 (s, 3H), 3.20 (d, 1H), 3.05 (m, 2H), 2.98 (d, 1H), 2.52 (d, 1H), 2.10 (d, 1H), 1.58 (s, 3H), 1.35 (s, 3H). MS (ESI): *m/e* 428 (MH⁺). HPLC purity: method A 98%, *t_R* 5.25 min; method B 99%, *t_R* 11.83 min.

1-[4-(5-Fluoro-2-methoxyphenyl)-2-hydroxy-4-methyl-2-(trifluoromethyl)pentyl]-2,3-dihydro-1H-quinolin-4-one (24). To a mixture of LAH (0.003 g) in anhydrous THF (0.8 mL) at 0–5 °C was added **11** (0.031 g). The mixture was stirred for 1 h and an additional 3–4 mg of LAH added. After 2 h the reaction was quenched with acetic acid, water, and ether. The organic layer was washed with water, saturated NaHCO₃, and brine and dried (MgSO₄). Removal of the volatiles in vacuo provided a residue which was purified with flash silica gel chromatography using 33% ethyl acetate in hexanes as the eluent. The product-rich fractions were collected and the volatiles removed in vacuo to provide 0.015 g of 1-[4-(5-fluoro-2-methoxyphenyl)-2-hydroxy-4-methyl-2-(trifluoromethyl)pentyl]-1,2,3,4-tetrahydroquinolin-4-ol. A mixture of this alcohol (0.015 g) and MnO₂ (0.2 g) in 2 mL of CH₂Cl₂ was stirred overnight, applied to a column of flash silica gel, and eluted with 25% ethyl acetate in hexanes. The product-rich fractions were collected and the volatiles removed in vacuo. Mass: 0.010 g. Mp: 132–134 °C. ¹H NMR (400 MHz, CDCl₃): δ 7.80 (d, 1H), 7.13 (m, 3H), 6.88 (m, 1H), 6.77 (m, 1H), 6.67 (m, 1H), 5.91 (d, 1H), 3.78 (s, 3H), 3.52 (d, 1H), 3.28 (m, 2H), 3.02 (d, 1H), 2.55 (m, 4H), 2.18 (d, 1H), 1.56 (s, 3H), 1.38 (s, 3H). IR (cm⁻¹): 1672, 1603. MS (ESI): *m/e* 440 (MH⁺). HPLC purity: method A 96%, *t_R* 4.74 min; method B 98%, *t_R* 10.82 min.

2-[(3,4-Dihydro-2H-quinolin-1-yl)methyl]-1,1,1-trifluoro-4-(5-fluoro-2-methoxyphenyl)-4-methylpentan-2-ol (25). To a mixture of **9** (0.21 g, 0.72 mmol) and 1,2,3,4-tetrahydroquinoline (0.096 g; 0.72 mmol) in methylene chloride (5 mL) was added flash silica gel (0.5 g). The volatiles were removed in vacuo. The residue was heated in a microwave at 150 °C for 4 min, applied to a column of flash silica gel, and eluted with 5% ethyl acetate in hexanes. The product-rich fractions were concentrated in vacuo. The residue was treated with ethereal HCl and the volatiles removed in vacuo. Trituration with hexanes and neutralization provided 0.06 g of the oily product. ¹H NMR (400 MHz, CDCl₃): δ 7.11 (dd, 1H), 6.87 (m, 3H), 6.73 (m, 2H), 6.60 (m, 1H), 5.97 (d, 1H), 3.73 (s, 3H), 3.27 (d, 1H), 3.15–2.90 (m, 3H), 2.67 (m, 2H), 2.55 (d, 1H), 2.12 (d, 1H), 1.57 (s, 3H), 1.40 (s, 3H). MS (ESI): *m/e* 426 (MH⁺). HPLC purity: method A 99%, *t_R* 4.21 min; method B 98%, *t_R* 13.07 min.

2-(Benzoimidazol-1-ylmethyl)-1,1,1-trifluoro-4-(5-fluoro-2-methoxyphenyl)-4-methylpentan-2-ol (26). A mixture of **9** (0.12 g, 0.41 mmol), benzimidazole (0.048 g; 0.41 mmol), and potassium *tert*-butoxide (0.1 mL of a 1 M solution in THF, 0.1 mmol) in DMSO (3 mL) was heated at 130 °C for 2 h, cooled to room temperature, and diluted with ethyl acetate and water. The organic

layer was washed with water and dried (MgSO₄). Removal of the volatiles provided a residue which was purified with silica gel chromatography using 80% ethyl acetate in petroleum ether as the eluent. The product-rich fractions were collected and the volatiles removed in vacuo. The residue was recrystallized from petroleum ether to provide 0.051 g of product. Mp: 180–182 °C. ¹H NMR (400 MHz, CDCl₃): δ 7.65 (m, 2H), 7.12 (m, 5H), 6.79 (m, 1H), 6.82 (m, 1H), 4.11 (s, 2H), 3.71 (s, 3H), 2.62 (d, 1H), 2.39 (d, 1H), 1.58 (s, 3H), 1.36 (s, 3H). MS (ESI): *m/e* 411 (MH⁺). HPLC purity: method A 94%, *t_R* 2.90 min; method B 96%, *t_R* 7.67 min.

1-[4-(5-Fluoro-2-methoxyphenyl)-2-hydroxy-4-methyl-2-(trifluoromethyl)pentyl]-1H-quinazolin-4-one (27). (a) A solution of 2-[2-(5-fluoro-2-methoxyphenyl)-2-methylpropyl]-2-(trifluoromethyl)oxirane (500 mg, 1.71 mmol) and 2-aminobenzamide (1.17 g, 8.56 mmol) in DMF (2.5 mL) was heated at 140 °C for 20 h. The reaction mixture was diluted with ether and washed with water and brine. The organic layer was dried (Na₂SO₄), filtered, and concentrated. Purification of the residue by column chromatography (15–30% ethyl acetate in hexanes) afforded 447 mg (61%) of 2-[4-(5-fluoro-2-methoxyphenyl)-2-hydroxy-4-methyl-2-(trifluoromethyl)pentyl]amino]benzamide as a white foam: ¹H NMR (400 MHz, DMSO-*d*₆): δ 8.19 (m, 1H, NH), 7.72 (s, 1H, NH), 7.51 (d, 1H, *J* = 7.9 Hz), 7.08 (m, 1H), 7.06 (m, 1H, NH), 6.98 (dd, 1H, *J* = 10.8, 3.0 Hz), 6.85 (m, 2H), 6.46 (m, 1H), 5.91 (d, 1H, *J* = 8.2 Hz), 5.87 (s, 1H, OH), 3.72 (s, 3H), 2.88 (m, 2H), 2.68 (m, 1H), 1.94 (d, 1H, *J* = 15.0 Hz), 1.49 (s, 3H), 1.33 (s, 3H). MS (ES): *m/e* 429 ([M + H]⁺). (b) To a solution of 2-[4-(5-fluoro-2-methoxyphenyl)-2-hydroxy-4-methyl-2-(trifluoromethyl)pentyl]amino]benzamide (106 mg, 0.247 mmol) in 6.0 mL of trimethyl orthoformate was added 0.1 mL of trifluoroacetic acid. After 1.5 h at room temperature, the reaction mixture was concentrated. Purification by column chromatography (70% EtOAc/hexanes) afforded 82.1 mg (76%) of the title compound as a white solid. Mp: 118–121 °C. ¹H NMR (400 MHz, MeOH-*d*₄): δ 8.20 (s, 1H), 8.16 (d, 1H, *J* = 8.0 Hz), 7.69 (m, 1H), 7.49 (m, 1H), 7.27 (d, 1H, *J* = 9.8 Hz), 7.08 (d, 1H, *J* = 8.6 Hz), 7.03 (m, 2H), 4.14 (m, 2H), 3.93 (s, 3H), 3.01 (d, 1H, *J* = 15.2 Hz), 2.16 (d, 1H, *J* = 15.2 Hz), 1.69 (s, 3H), 1.47 (s, 3H). MS (ES): *m/e* 439 ([M + H]⁺). HPLC purity: method A 99%, *t_R* 3.21 min; method B 98%, *t_R* 7.97 min.

1-[4-(5-Fluoro-2-methoxyphenyl)-2-hydroxy-4-methyl-2-(trifluoromethyl)pentyl]-1H-[1,5]naphthyridin-4-one (28). Mp: 193–195 °C. ¹H NMR (400 MHz, MeOH-*d*₄): δ 8.64 (m, 1H), 7.78 (d, 1H, *J* = 7.9 Hz), 7.54 (m, 2H), 7.28 (d, 1H, *J* = 9.8 Hz), 7.02 (m, 2H), 6.37 (d, 1H, *J* = 7.9 Hz), 4.23 (d, 1H, *J* = 16.0 Hz), 4.11 (d, 1H, *J* = 16.0 Hz), 3.91 (s, 3H), 2.95 (d, 1H, *J* = 15.2 Hz), 2.15 (d, 1H, *J* = 15.2 Hz), 1.68 (s, 3H), 1.47 (s, 3H). FTIR (neat): 1625, 1584 cm⁻¹. MS (ES): *m/e* 440 ([M + H]⁺).

1-[4-(5-Fluoro-2-methoxyphenyl)-2-hydroxy-4-methyl-2-(trifluoromethyl)pentyl]-1H-[1,6]naphthyridin-4-one (29). Mp: 229–230 °C. ¹H NMR (400 MHz, MeOH-*d*₄): δ 9.28 (s, 1H), 8.43 (d, 1H, *J* = 6.4 Hz), 7.77 (d, 1H, *J* = 8.0 Hz), 7.29 (m, 1H), 7.03 (m, 2H), 6.94 (d, 1H, *J* = 6.4 Hz), 6.27 (d, 1H, *J* = 8.0 Hz), 4.13 (d, 1H, *J* = 15.9 Hz), 4.05 (d, 1H, *J* = 15.9 Hz), 3.92 (s, 3H), 2.98 (d, 1H, *J* = 15.2 Hz), 2.14 (d, 1H, *J* = 15.2 Hz), 1.69 (s, 3H), 1.47 (s, 3H). FTIR (neat): 1642, 1587 cm⁻¹. MS (ES): *m/e* 439 ([M + H]⁺). HPLC purity: method A 99%, *t_R* 2.59 min; method B 99%, *t_R* 6.91 min.

1-(2-Hydroxy-4-methyl-4-phenyl-2-(trifluoromethyl)pentyl)-1H-quinolin-4-one (30). Mp: 80–82 °C. ¹H NMR (400 MHz, CDCl₃): δ 8.30 (d, 1H, *J* = 7.3 Hz), 7.53 (m, 1H), 7.39 (m, 5H), 7.26 (m, 2H), 7.18 (d, 1H, *J* = 8.7 Hz), 6.09 (d, 1H, *J* = 7.9 Hz), 4.08 (d, 1H, *J* = 15.8 Hz), 3.91 (d, 1H, *J* = 15.8 Hz), 3.71 (s, 1H, OH), 2.39 (d, 1H, *J* = 15.4 Hz), 2.25 (d, 1H, *J* = 15.4 Hz), 1.61 (s, 3H), 1.37 (s, 3H). MS (ES): *m/e* 390 ([M + H]⁺). HPLC purity: method A 99%, *t_R* 3.25 min; method B 99%, *t_R* 7.60 min.

1-[2-Hydroxy-4-(2-hydroxyphenyl)-4-methyl-2-(trifluoromethyl)pentyl]-1H-quinolin-4-one (31). Mp: 157 °C. ¹H NMR (400 MHz, MeOH-*d*₄): δ 8.6 (d, 1H), 8.45 (d, 1H), 7.9 (t, 1H), 7.75 (t, 1H), 7.55 (d, 1H), 7.5 (d, 1H), 7.18 (t, 1H), 7.05 (d, 1H), 6.98 (t, 1H), 6.85 (d, 1H), 3.25 (m, 2H), 4.6 (s, 2H), 2.2 (d, 1H), 1.73 (s,

3H), 1.55 (s, 3H). MS (ESI): *m/e* 406 (M⁺), 404 (M⁻). HPLC purity: method A 92%, *t_R* 3.02 min; method B 85%, *t_R* 7.08 min.

1-[2-Hydroxy-4-methyl-4-*o*-tolyl-2-(trifluoromethyl)pentyl]-1*H*-quinolin-4-one (32). Mp: 174 °C. ¹H NMR (400 MHz, CDCl₃): δ 8.26 (m, 1H), 7.52 (m, 2H), 7.4 (d, 1H), 7.3–7.15 (m, 4H), 7.08 (d, 1H), 6.1 (d, 1H), 4.05 (q, 2H), 2.5 (s, 3H), 2.4 (q, 2H), 1.7 (s, 3H), 1.48 (s, 3H). MS (ESI): *m/e* 404 (M⁺). HPLC purity: method A 96%, *t_R* 3.44 min; method B 99%, *t_R* 8.03 min.

1-[4-(5-Fluoro-2-methylphenyl)-2-hydroxy-4-methyl-2-(trifluoromethyl)pentyl]-1*H*-quinolin-4-one (33). Mp: 103–105 °C. ¹H NMR (400 MHz, CDCl₃): δ 8.16 (dd, 1H, *J* = 8.1, 1.5 Hz), 7.50 (m, 1H), 7.37 (d, 1H, *J* = 7.8 Hz), 7.28 (m, 1H), 7.23 (m, 1H), 7.07 (m, 2H), 6.87 (m, 1H), 6.01 (d, 1H, *J* = 7.8 Hz), 4.52 (s, 1H, OH), 4.10 (d, 1H, *J* = 15.7 Hz), 3.95 (d, 1H, *J* = 15.7 Hz), 2.50 (s, 3H), 2.47 (d, 1H, *J* = 15.6 Hz), 2.33 (d, 1H, *J* = 15.6 Hz), 1.72 (s, 3H), 1.48 (s, 3H). MS (ES): *m/e* 422 ([M + H]⁺). HPLC purity: method A 98%, *t_R* 3.47 min; method B 99%, *t_R* 8.08 min.

1-[2-Hydroxy-4-(2-hydroxy-5-methylphenyl)-4-methyl-2-(trifluoromethyl)pentyl]-1*H*-quinolin-4-one (34). Mp: 160–161 °C. ¹H NMR (400 MHz, MeOH-*d*₄): δ 8.21 (d, 1H), 7.73 (d, 1H), 7.52 (t, 1H), 7.30 (m, 2H), 7.13 (d, 1H), 6.94 (d, 1H), 6.72 (d, 1H), 6.19 (d, 1H) 4.27 (d, 1H), 4.13 (d, 1H), 3.15 (d, 1H), 2.29 (s, 3H), 2.13 (d, 1H), 1.69 (s, 3H), 1.50 (s, 3H). MS (ESI): *m/e* 419 (M⁺).

1-[2-Hydroxy-4-(5-methoxy-2-methylphenyl)-4-methyl-2-(trifluoromethyl)pentyl]-1*H*-quinolin-4-one (35). Mp: 196–198 °C. ¹H NMR (400 MHz, CDCl₃): δ 8.37 (d, 1H), 7.55 (t, 1H), 7.4 (d, 1H), 7.3 (t, 1H), 7.27–7.08 (m, 3H), 6.72 (d, 1H), 6.15 (d, 1H), 4.1 (q, 2H), 3.8 (s, 3H), 2.98 (s, 1H), 2.4 (s, 3H), 2.38 (q, 2H), 1.65 (s, 3H), 1.43 (s, 3H). MS (ESI): *m/e* 434 (M⁺). HPLC purity: method A 98%, *t_R* 3.43 min; method B 98%, *t_R* 7.96 min.

1-[2-Hydroxy-4-(5-hydroxy-2-methylphenyl)-4-methyl-2-(trifluoromethyl)pentyl]-1*H*-quinolin-4-one (36). Mp: 125–127 °C. ¹H NMR (400 MHz, MeOH-*d*₄): δ 8.28 (d, 1H), 7.83 (d, 1H), 7.68 (t, 1H), 7.4 (t, 1H), 7.29 (d, 1H), 7.16 (d, 1H), 7.06 (d, 1H), 6.62 (m, 1H), 6.39 (d, 1H), 4.16 (q, 2H), 2.72 (d, 1H), 2.58 (s, 3H), 2.18 (d, 1H), 1.78 (s, 3H), 1.5 (s, 3H). MS (ESI): *m/e* 421 (M⁺). HPLC purity: method A 97%, *t_R* 2.89 min; method B 94%, *t_R* 6.85 min.

1-[4-(4-Fluoro-2-hydroxyphenyl)-2-hydroxy-4-methyl-2-(trifluoromethyl)pentyl]-1*H*-quinolin-4-one (37). Mp: 293–295 °C. ¹H NMR (400 MHz, DMSO-*d*₆): δ 10.3 (s, 1H, OH), 8.07 (d, 1H, *J* = 7.5 Hz), 7.61 (d, 1H, *J* = 7.8 Hz), 7.53 (m, 1H), 7.34 (m, 1H), 7.27 (m, 1H), 7.13 (d, 1H, *J* = 8.6 Hz), 6.63 (m, 2H), 6.22 (s, 1H, OH), 5.97 (d, 1H, *J* = 7.8 Hz), 4.05 (d, 1H, *J* = 16.2 Hz), 3.94 (d, 1H, *J* = 16.2 Hz), 2.99 (d, 1H, *J* = 15.0 Hz), 2.03 (d, 1H, *J* = 15.0 Hz), 1.61 (s, 3H), 1.38 (s, 3H). MS (ES): *m/e* 424 ([M + H]⁺). HPLC purity: method A 95%, *t_R* 3.14 min; method B 96%, *t_R* 7.26 min.

1-[4-(2,3-Dihydrobenzofuran-7-yl)-2-hydroxy-4-methyl-2-(trifluoromethyl)pentyl]-1*H*-quinolin-4-one (38). Mp: 187–188 °C. ¹H NMR (400 MHz, DMSO-*d*₆): δ 8.18 (d, 1H), 7.70 (m, 2H), 7.38 (7, 1H), 7.29 (m, 3H), 6.94 (t, 1H), 6.32 (s, 1H), 6.08 (d, 1H), 4.68 (t, 2H), 4.05 (dd, 2H), 3.22 (t, 1H), 2.88 (d, 1H), 2.12 (d, 1H), 1.70 (s, 3H), 1.43 (s, 3H). FTIR neat (cm⁻¹): 1624, 1610. MS (ES): *m/e* 432 ([M + H]⁺). HPLC purity: method A 97%, *t_R* 3.38 min; method B 97%, *t_R* 8.07 min; method C 98%, *t_R* 10.50 min.

1-[4-(2,3-Dihydrobenzofuran-7-yl)-2-hydroxy-4-methyl-2-(trifluoromethyl)pentyl]-3,5-dimethyl-1*H*-pyridin-4-one (39). Mp: 237–238 °C. ¹H NMR (400 MHz, MeOH-*d*₄): δ 7.35 (s, 2H), 7.17 (d, 1H, *J* = 7.8 Hz), 7.13 (d, 1H, *J* = 7.3 Hz), 6.85 (m, 1H), 4.59 (m, 2H), 3.74 (d, 1H, *J* = 15.1 Hz), 3.50 (d, 1H, *J* = 15.1 Hz), 3.18 (m, 2H), 2.92 (d, 1H, *J* = 15.3 Hz), 1.99 (d, 1H, *J* = 15.3 Hz), 1.95 (s, 6H), 1.64 (s, 3H), 1.38 (s, 3H). MS (ES): *m/e* 410 ([M + H]⁺). HPLC purity: method A 99%, *t_R* 2.81 min; method B 98%, *t_R* 7.30 min.

1-[4-(5-Fluoro-2-methylphenyl)-2-hydroxy-4-methyl-2-(trifluoromethyl)pentyl]-1*H*-[1,6]naphthyridin-4-one (40). Mp: 253–255 °C. ¹H NMR (400 MHz, MeOH-*d*₄): δ 9.27 (s, 1H), 8.45 (d, 1H, *J* = 6.3 Hz), 7.76 (d, 1H, *J* = 8.0 Hz), 7.38 (dd, 1H, *J* = 2.7,

12.1 Hz), 7.21 (dd, 1H, *J* = 6.6, 8.3 Hz), 7.00 (d, 1H, *J* = 6.3 Hz), 6.93 (m, 1H), 6.27 (d, 1H, *J* = 8.0 Hz), 4.08 (m, 2H), 2.67 (d, 1H, *J* = 15.6 Hz), 2.62 (s, 3H), 2.23 (d, 1H, *J* = 15.6 Hz), 1.77 (s, 3H), 1.54 (s, 3H). MS (ES): *m/e* 423 ([M + H]⁺). HPLC purity: method A 99%, *t_R* 2.44 min; method B 99%, *t_R* 6.42 min.

1-[4-(5-Fluoro-2-methylphenyl)-2-hydroxy-4-methyl-2-(trifluoromethyl)pentyl]-3,5-dimethyl-1*H*-pyridin-4-one (41). Mp: 205–207 °C. ¹H NMR (400 MHz, MeOH-*d*₄): δ 7.38 (s, 2H), 7.25 (m, 1H), 7.16 (m, 1H), 6.87 (m, 1H), 3.71 (d, 1H, *J* = 15.0 Hz), 3.59 (d, 1H, *J* = 15.0 Hz), 2.64 (d, 1H, *J* = 15.6 Hz), 2.55 (s, 3H), 2.11 (d, 1H, *J* = 15.6 Hz), 1.95 (s, 6H), 1.71 (s, 3H), 1.48 (s, 3H). MS (ES): *m/e* 401 ([M + H]⁺). HPLC purity: method A 99%, *t_R* 2.78 min; method B 99%, *t_R* 7.21 min.

Nuclear Receptor Assays. GR, PR, and MR binding assays were performed in a fluorescence polarization microplate format that measures competition for binding to the nuclear receptor between a test compound and a fluorescently labeled receptor ligand, or probe. The probes used for the assays were as follows: GR and MR assays, 5 nM tetramethylrhodamine-labeled dexamethasone; PR assay, 5 nM tetramethylrhodamine-labeled RU-486. For GR and MR assays, receptors present in lysates of baculovirus-infected insect cells co-infected with receptor, HSP-70, HSP-90, and p23 were used. For PR binding assays, lysates were generated from insect cells infected with receptor-containing baculovirus alone. Binding reactions consisted of lysate, the test compound, and the probe combined in an assay buffer containing 10 mM TES, 50 mM KCl, 20 mM Na₂MoO₄·2H₂O, 1.5 mM EDTA, 0.04% (w/v) CHAPS, 10% (v/v) glycerol, and 1 mM dithiothreitol, pH 7.4. Lysates containing GR, PR, and MR were diluted into the assay 300-fold, 13-fold, and 17-fold in the respective binding reactions. The DMSO concentration in all binding reactions was 1% (v/v). Following 1 h of incubation in the dark at room temperature, the fluorescence polarization signal was measured using a Molecular Devices Analyst plate reader with excitation and emission filters of 550 and 580 nm selected and with a 561 nm dichroic mirror installed. The positive control FP signal was measured in assay wells containing binding reactions without inhibitor. The fluorescence polarization signal produced by maximal inhibition (background control) was determined using the signals from wells containing 2 μM concentrations of a standard inhibitor for each receptor: dexamethasone for GR and MR and RU-486 for PR. Fluorescence polarization signals from duplicate 11-point concentration–response curves were fitted to a 4-parameter logistic equation to determine IC₅₀ values.

Cellular Assays. The fibroblast IL-6 assay measures the ability of test compounds to inhibit the elaboration of IL-6 by human foreskin fibroblasts following stimulation by IL-1 in vitro. Human foreskin fibroblasts (ATCC no. CRL-2429) were grown in Iscove's medium supplemented with 10% (v/v) charcoal/dexamethasone-treated fetal bovine serum and plated at 20000 cells/well 2 days prior to the assay. On the day of the assay, the medium was replaced, followed by the addition of the test compound (0.4% DMSO final assay concentration) and recombinant human IL-1 (final concentration 1 ng/mL). After incubation at 37 °C for 18–24 h, IL-6 in the tissue culture medium was quantitated using standard electrochemiluminescence, DELFIA, or ELISA methods. Test compound IC₅₀ values were determined by fitting the data from duplicate 11-point concentration–response curves to a 4-parameter logistic equation. In this assay, IL-6 inhibition is considered a measure of the agonist response of the glucocorticoid receptor, and dexamethasone is considered to possess 100% efficacy.

The fibroblast aromatase assay measures the ability of test compounds to induce aromatase activity in human foreskin fibroblasts, as indicated by the production of β-estradiol in the presence of exogenously added testosterone. Human foreskin fibroblasts (ATCC no. CRL-2429) were grown in Iscove's medium supplemented with 10% (v/v) charcoal/dexamethasone-treated fetal bovine serum and plated at 10000 cells/well 5 days prior to the assay. On the day of the assay, the medium was replaced, followed by the addition of the test compound (0.4% DMSO final assay

concentration) and testosterone (final concentration 1 μ M). After incubation at 37 °C for 18–24 h, estradiol was quantitated in the tissue culture medium using a commercial ELISA (ALPCO no. 020-DR-2693). Test compound EC₅₀ values were determined by fitting the data from duplicate 11-point concentration–response curves to a 4-parameter logistic equation. For test compound comparison, dexamethasone was considered to possess 100% efficacy in this assay.

HeLa MMTV transactivation assay measures the ability of test compounds to activate MMTV promoter in HeLa cells stably transfected with MMTV luciferase construct. HeLa MMTV cells were grown in DMEM medium supplemented with 10% (v/v) fetal bovine serum (Hyclone), 100 U/mL penicillin, 100 μ g/mL streptomycin, 2 mM L-glutamine, and 300 μ g/mL genetecin. The day prior to assay the cells were plated at 25000 cells/well in 96-well white clear bottom cell culture plates in DMEM medium supplemented with 3% (v/v) FBS, 100 U/mL penicillin, 100 μ g/mL streptomycin, and 2 mM L-glutamine. On the day of the assay, the medium was replaced, followed by addition of the test compound (0.2% DMSO final assay concentration). Positive control wells received 1 μ M dexamethasone and represent 100% induction, while negative control wells received vehicle only and represent background. After final addition of the compounds the plates were incubated for 6 h at 37 °C and 5% CO₂. After the incubation period luminescence was detected upon cell lysis with Steady Glow luciferase reagent (Promega no. E2520). Activation of MMTV promoter by test compounds is expressed in percentage relative to the positive control. Test compound EC₅₀ values were determined by nonlinear curve fitting of the data from duplicate eight-point concentration–response curves.

In Vivo LPS Challenge Assay. Female Balb/c mice, weighing approximately 20 g, were used. Mice were administered **1a**, the test compound, and vehicle in cremophor (po) approximately 60 min prior to LPS/D-gal administration. The volume of oral gavage was 0.15 mL. Then the mice were administered LPS (*Escherichia coli* LPS 055:85, 1.0 μ g/mouse) plus D-gal (50 mg/kg) intravenously in 0.2 mL of pyrogen-free saline. One hour after LPS/D-gal administration, each mouse was anesthetized and bled by cardiac puncture and the blood collected for serum TNF- α and compound levels. Blood samples were centrifuged at 2500 rpm for 10–15 min, the serum was decanted, and the samples were stored frozen at –70 °C until transfer either for TNF- α determination or to Drug Metabolism and Pharmacokinetics for plasma concentration analysis by HPLC. The concentration of TNF- α in the serum was measured by a commercially available ELISA kit (R&D Systems, Minneapolis, MN). ELISA was performed according to the manufacturer's assay procedure. All samples were assayed in duplicate.

Acknowledgment. We thank Gayle DeBaun for help in the preparation of this manuscript.

References

- Gupta, R.; Jindal, D. P.; Kumar, G. Corticosteroids: the mainstay in asthma therapy. *Bioorg. Med. Chem.* **2004**, *12*, 6331–6342.
- Buttgereit, F.; Saag, K. G.; Cutolo, M.; da Silva, J. A.; Bijlsma, J. W. The molecular basis for the effectiveness, toxicity, and resistance to glucocorticoids: focus on the treatment of rheumatoid arthritis. *Scand. J. Rheumatol.* **2005**, *34*, 14–21.
- Zhou, J.; Cidlowski, J. A. The human glucocorticoid receptor: one gene, multiple proteins and diverse responses. *Steroids* **2005**, *70*, 407–417.
- Resche-Rigon, M.; Gronemeyer, H. Therapeutic potential of selective modulators of nuclear receptor action. *Curr. Opin. Chem. Biol.* **1998**, *2*, 501–507.
- Adcock, I. M. Molecular mechanisms of glucocorticosteroid actions. *Pulm. Pharmacol. Ther.* **2000**, *13*, 115–126.
- Heck, S.; Kullmann, M.; Gast, A.; Ponta, H.; Rahmsdorf, H. J.; Herrlich, P.; Cato, A. C. A distinct modulating domain in glucocorticoid receptor monomers in the repression of activity of the transcription factor AP-1. *EMBO J.* **1994**, *13*, 4087–4095.
- Schacke, H.; Docke, W. D.; Asadullah, K. Mechanisms involved in the side effects of glucocorticoids. *Pharmacol. Ther.* **2002**, *96*, 23–43.
- Katzenellenbogen, J. A.; Katzenellenbogen, B. S. Nuclear hormone receptors: ligand-activated regulators of transcription and diverse cell responses. *Chem. Biol.* **1996**, *3*, 529–536.
- Burnstein, K. L.; Cidlowski, J. A. The down side of glucocorticoid receptor regulation. *Mol. Cell. Endocrinol.* **1992**, *83*, C1–C8.
- Coghlan, M. J.; Elmore, S. W.; Kym, P. R.; Kort, M. E. Selective Glucocorticoid Receptor Modulators. In *Annual Reports in Medicinal Chemistry*; Doherty, A. M., Ed.; Academic Press: New York, 2002; pp 167–176.
- Schacke, H.; Rehwinkel, H.; Asadullah, K.; Cato, A. C. Insight into the molecular mechanisms of glucocorticoid receptor action promotes identification of novel ligands with an improved therapeutic index-amethasone. *Exp. Dermatol.* **2006**, *15*, 565–573.
- Belvisi, M. G.; Brown, T. J.; Wicks, S.; Foster, M. L. New Glucocorticosteroids with an improved therapeutic ratio? *Pulm. Pharmacol. Ther.* **2001**, *14*, 221–227.
- Miner, J. N. Designer glucocorticoids. *Biochem. Pharmacol.* **2002**, *64*, 355–361.
- Schacke, H.; Schottelius, A.; Docke, W. D.; Strehlke, P.; Jaroch, S.; Schmees, N.; Rehwinkel, H.; Hennekes, H.; Asadullah, K. Dissociation of transactivation from transrepression by a selective glucocorticoid receptor agonist leads to separation of therapeutic effects from side effects. *Proc. Natl. Acad. Sci. U.S.A.* **2004**, *101*, 227–232.
- Barker, M.; Clackers, M.; Demaine, D. A.; Humphreys, D.; Johnston, M. J.; Jones, H. T.; Pacquet, F.; Pritchard, J. M.; Salter, M.; Shanahan, S. E.; Skone, P. A.; Vinader, V. M.; Uings, I.; McLay, I. M.; Macdonald, S. J. Design and synthesis of new nonsteroidal glucocorticoid modulators through application of an "agreement docking" method. *J. Med. Chem.* **2005**, *48*, 4507–4510.
- Bledsoe, R. K.; Lambert, M. H.; Montana, V. G.; Stewart, E. L.; Xu, E. H. Structure of a Glucocorticoid Ligand Binding Domain Comprising an Expanded Binding Pocket, and Methods Using Nuclear Receptors Structure for Drug Design. *Eur. Pat. Appl.* 1375517, 2004.
- Betageri, R.; Zhang, Y.; Zindell, R. M.; Kuzmich, D.; Kirrane, T. M.; Bentzien, J.; Cardozo, M.; Capolino, A. J.; Fadra, T. N.; Nelson, R. M.; Paw, Z.; Shih, D. T.; Shih, C. K.; Zuvella-Jelaska, L.; Nabozny, G.; Thomson, D. S. Trifluoromethyl group as a pharmacophore: effect of replacing a CF₃ group on binding and agonist activity of a glucocorticoid receptor ligand. *Bioorg. Med. Chem. Lett.* **2005**, *15*, 4761–4769.
- Abraham, M. H.; Duce, P. P.; Prior, D. V.; Barratt, D. G.; Morris, J. J.; Taylor, P. J. Hydrogen bonding. Part 9. Solute proton donor and proton acceptor scales for use in drug design. *J. Chem. Soc., Perkin Trans. 2* **1989**, 1355–1375.
- Bekkali, Y.; Cardozo, M.; Kirrane, T. M.; Kuzmich, D.; Proudfoot, J. R.; Takahashi, H.; Thomson, D.; Wang, J.; Zindell, R.; Harcken, C. H. J. J.; Razavi, H. Glucocorticoid Mimetics, Methods of Making Them, Pharmaceutical Compositions, and Uses Thereof. WO 03/082787, 2003.
- Proudfoot, J. R.; Regan, J. R.; Thomson, D. S.; Kuzmich, D.; Lee, T. W.-H.; Hammach, A.; Ralph, M. S.; Zindell, R.; Bekkali, Y. 1-Propanol and 1-Propylamine Derivatives and Their Use as Glucocorticoid Ligands. WO 04/063163, 2004.
- Harper, N.; Chignell, C.; Kirk, G. F. Synthesis of some N-substituted 3,5-dimethyl-4-piperidinols and their derivatives as potential analgesics. *J. Med. Chem.* **1964**, *7*, 726–728.
- McCabe, P. H.; Milne, N. J.; Sim, G. A. Conformational study of bridgehead lactams. Preparation and x-ray structural analysis of 1-azabicyclo[3.3.1]nonane-2,6-dione. *J. Chem. Soc., Perkin Trans. 2* **1989**, *10*, 1459–1462.
- Briefly, GR, PR, and MR binding assays were performed in a fluorescence polarization format that measures competition for binding to the nuclear receptor, present in lysates of baculovirus-infected insect cells, between a test compound and a fluorescently labeled receptor ligand, or probe. IC₅₀ values were determined by fitting the fluorescence polarization signal data to a four-parameter logistic equation. All IC₅₀ values shown represent the mean of at least two independent determinations. Repeated testing of reference compounds in these assays demonstrates typical IC₅₀ standard deviations of 20–40% about the mean. See the Experimental Section for complete details.
- Waage, A.; Slupphaug, G.; Shalaby, R. Glucocorticoids inhibit the production of IL6 from monocytes, endothelial cells and fibroblasts. *Eur. J. Immunol.* **1990**, *20*, 2439–2443.
- IL-6 levels were quantitated in tissue culture supernatants 18–24 h following compound addition and IL-1 stimulation, and compound IC₅₀ values were determined by fitting the data from duplicate 11-point concentration–response curves to a 4-parameter logistic equation. In this assay, IL-6 inhibition is considered a measure of the agonist response of the glucocorticoid receptor, and dexamethasone is considered to possess 100% efficacy. All IC₅₀ values shown

represent the mean of at least two independent determinations. Repeated testing of reference compounds in these assays demonstrates typical IC_{50} standard deviations of 20–30% about the mean. See the Experimental Section for complete details.

- (26) The assay measures the ability of test compounds to induce aromatase activity in human foreskin fibroblasts, as indicated by the production of β -estradiol in the presence of exogenously added testosterone. β -Estradiol levels were quantitated in the tissue culture media 18–24 h following test compound and testosterone addition, and test compound EC_{50} values were determined by fitting data from duplicate 11-point concentration–response curves to a 4-parameter logistic equation. For test compound comparison, dexamethasone was considered to possess 100% efficacy in this assay. All EC_{50} values shown represent the mean of at least two independent determinations. Repeated testing of reference compounds in these assays demonstrates typical EC_{50} standard deviations of 30–50% about the mean. See the Experimental Section for complete details.
- (27) HeLa cells stably transfected with MMTV luciferase construct are incubated in the presence of the test compounds for 6 h. After the incubation period, luminescence is detected in cell lysates. Test compound EC_{50} values are determined by nonlinear curve fitting of the data from duplicate eight-point concentration–response curves. Repeated testing of reference compounds in these assays demonstrates a 30% coefficient of variation. See the Experimental Section for complete details.
- (28) Thompson, C. F.; Quraishi, N.; Ali, A.; Tata, J. R.; Hammond, M. L.; Balkovec, J. M.; Einstein, M.; Ge, L.; Harris, G.; Kelly, T. M.; Mazur, P.; Pandit, S.; Santoro, J.; Sitlani, A.; Wang, C.; Williamson, J.; Miller, D. K.; Yamin, T. T.; Thompson, C. M.; O'Neill, E. A.; Zaller, D.; Forrest, M. J.; Carballo-Jane, E.; Luell, S. Novel heterocyclic glucocorticoids: in vitro profile and in vivo efficacy. *Bioorg. Med. Chem. Lett.* **2005**, *15*, 2163–2167.
- (29) Smith, C. J.; Ali, A.; Balkovec, J. M.; Graham, D. W.; Hammond, M. L.; Patel, G. F.; Rouen, G. P.; Smith, S. K.; Tata, J. R.; Einstein, M.; Ge, L.; Harris, G. S.; Kelly, T. M.; Mazur, P.; Thompson, C. M.; Wang, C. F.; Williamson, J. M.; Miller, D. K.; Pandit, S.; Santoro, J. C.; Sitlani, A.; Yamin, T. T.; O'Neill, E. A.; Zaller, D. M.; Carballo-Jane, E.; Forrest, M. J.; Luell, S. Novel ketal ligands for the glucocorticoid receptor: in vitro and in vivo activity. *Bioorg. Med. Chem. Lett.* **2005**, *15*, 2926–2931.
- (30) Bourguet, W.; Germain, P.; Gronemeyer, H. Nuclear receptor ligand-binding domains: three-dimensional structures, molecular interactions and pharmacological implications. *Trends Pharmacol. Sci.* **2000**, *21*, 381–388.
- (31) Bledsoe, R. K.; Stewart, E. L.; Pearce, K. H. Structure and function of the glucocorticoid receptor ligand binding domain. *Vitam. Horm.* **2004**, *68*, 49–91.
- (32) Berkovitz, G. D.; Bisat, T.; Carter, K. M. Aromatase activity in microsomal preparations of human genital skin fibroblasts: influence of glucocorticoids. *J. Steroid Biochem.* **1989**, *33*, 341–347.
- (33) Vayssiere, B. M.; Dupont, S.; Choquart, A.; Petit, F.; Garcia, T.; Marchandeu, C.; Gronemeyer, H.; Resche-Rigon, M. Synthetic glucocorticoids that dissociate transactivation and AP-1 transrepression exhibit antiinflammatory activity in vivo. *Mol. Endocrinol.* **1997**, *11*, 1245–1255.

JM061273T